CrossMark

A Numerical Assessment of Anodic Large Bubble on Horizontal Current in Metal Pad of Aluminum Electrolytic Cells

WENJU TAO,[1,2,3] TUOFU LI,[1] ZHAOWEN WANG,[1,4] BINGLIANG GAO,[1] ZHONGNING SHI,[1] XIANWEI HU,[1] and JIANZHONG CUI[1,2]

1.—School of Materials and Metallurgy, Northeastern University, Shenyang 110819, China. 2.—Key Laboratory of Electromagnetic Processing of Materials, Ministry of Education, Northeastern University, Shenyang 110819, China. 3.—e-mail: 2004taowenju@gmail.com. 4.—e-mail: wangzw@smm.neu.edu.cn

This study reports on an assessment of an anodic large bubble on the horizontal current in the metal pad of an aluminum electrolytic cell using a numerical model. The effects of bubble position and coverage on the horizontal current were investigated. The predicted results show that large bubbles have a significant impact on the horizontal current: The horizontal current with a bubble located at the right part of carbon anode (cell side) will provide coverage of 33.3% up to 30,174 A m^{-2} compared with 13,001 A m^{-2} without bubble at the upper surface of metal pad; For a fixed bubble position, the maximum horizontal current increases and the location of the maximum horizontal current density shifts from the anode center to the cell center with increasing the bubble coverage; The bubble position (for a fixed bubble coverage) significantly influences horizontal current. When the bubble varies from the cell center to the cell side, the maximum horizontal current density will increase and the location of the maximum horizontal current density shifts from the cell center to the cell side. When the whole anode is covered with a large bubble, a large inward horizontal current appears on the cell side and the maximum inward horizontal current can reach up to 35,575 A m^{-2}.

INTRODUCTION

Industrial primary aluminum is produced by the Hall–Heroult electrolytic reduction process in an aluminum electrolytic cell, with electrolysis of dissolved alumina in a molten electrolyte (molten cryolite and additives such as CaF_2, MgF_2 etc.). The aluminum electrolytic cell is the only equipment for the production of aluminum in an industrial setting. Although the cell designs have undergone substantial improvements over time, the cells are still similar to the earliest cell designs, as shown in Fig. 1.

In a cell, the direct electric current flows vertically downward through the anode, passes through the electrolyte, metal pad (molten aluminum layer), and cathode carbon block and flows horizontally out of the cell by collector bars to the cathode busbar, which is connected to the risers of the next cell. Notably, the current flows through the least resistance. The metal pad has a very high electrical conductivity, approximately 4×10^4 S cm^{-1}, four orders of magnitude greater than the electrolyte, of which is approximately 2 S cm^{-1}. So once the currents enter the molten aluminum layer, they will take long paths in the molten aluminum layer toward areas on the cathode carbon block close to the outlet of current, as shown in Fig. 2. In other words, horizontal components of current, so called horizontal current (HC), establish themselves in the metal pad. The horizontal current interacting with vertical magnetic forces provokes vortices and stirring, fluctuation of the molten aluminum,[1] causing some adverse effects on cells such as reduction of the anode cathode distance, which is closely related to the cell voltage because of the smaller electrical conductivity of electrolyte, and back reaction of the molten aluminum. After recognizing the adverse effects of the horizontal current on the energy consumption and current efficiency, many studies have been conducted to investigate the factors that affect the horizontal current: It is found that the

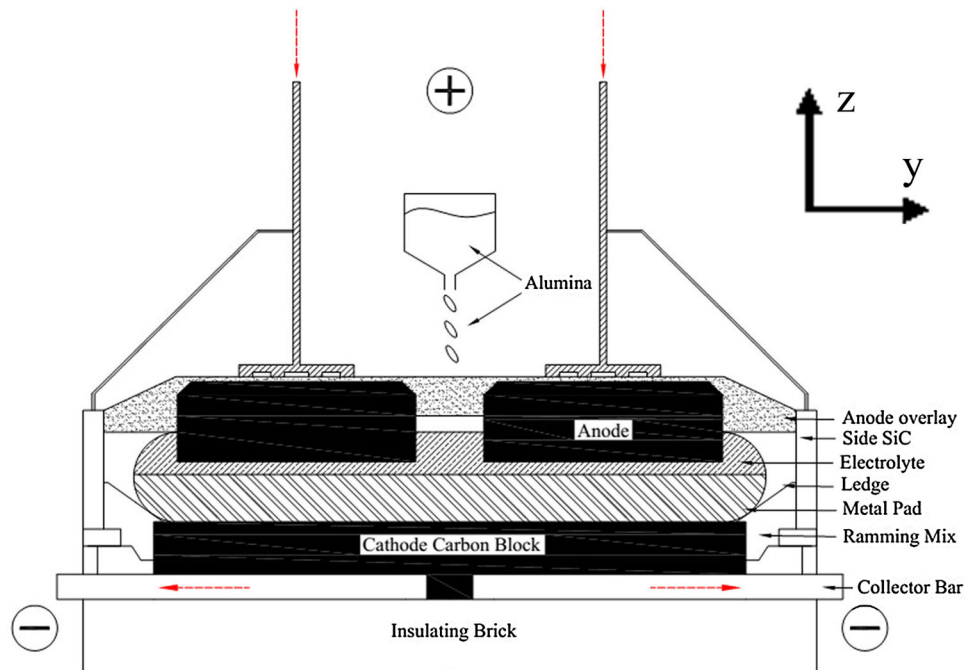(Published online December 18, 2015)

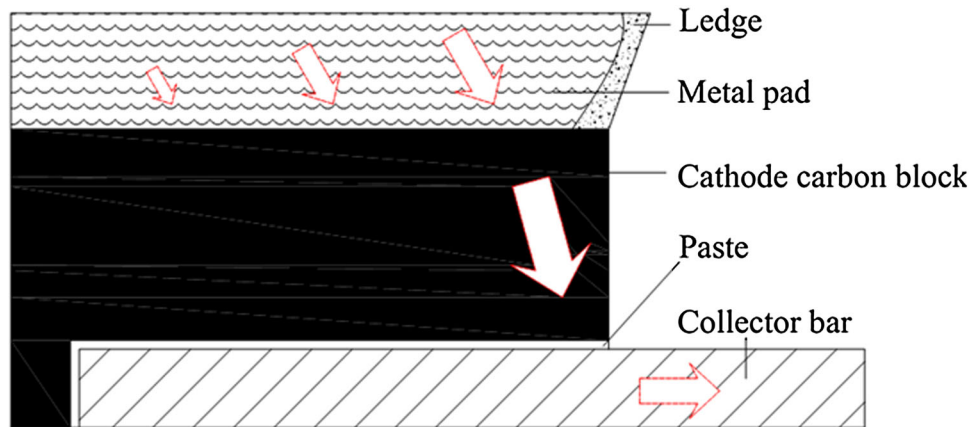Fig. 1. Schematic representation of an aluminum electrolytic cell.

Fig. 2. Schematic representation of current path in cathode.

horizontal current is greatly influenced by the structure of cathode,[2] so many cell designs, by modifying the cathode carbon[3–6] or collector bars,[7–13] have been proposed to render the horizontal current more uniform; Increasing the metal height will cause a reduction in the maximum HC[14–16]; With increasing ledge, the inward flowing current increase[17,18]; Moreover, both the side wall and the sludge in the cell[19] are also important factors.

The works mentioned earlier gave relative accurate descriptions of the horizontal current and the influence factor in cells. However, the anodic large bubble, a critical factor, was ignored in these works. The present work studied the impact of the anodic large bubble on current distribution, especially

horizontal current, in the metal pad by using a finite element method. The effects of the bubble position and coverage on horizontal current were also investigated.

THE ANODIC GAS BUBBLE LAYER

In a cell, the anode carbon is oxidized, forming the gas (CO and CO_2) underside of the large horizontal carbon anodes. The gas coalesces into bubbles that then travel to, and are released at, the anode edge, significantly affecting the cell voltage and current efficiency.[20] Because of the poor electrical conductivity, the gas bubbles induce an extra voltage drop which range from 0.15 V to 0.35 V, out of a total cell voltage of 4.0–4.6 V, a significant amount of extra

Table I. Parameters of bubble in cells

Parameter	Method	References
Thickness of the bubble layer (cm)		
0.4–0.6 (range up to 0.71 cm)	Physical model	Aaberg[33]
0.5	Physical model	Fortin[25]
0.5	Measurements in industrial cells	Haupin[34]
0.5	Physical model	Dewing[35]
0.4	Physical model	Xue[29]
The bubble profile		
Large bubbles: longitudinal dimension of the bubbles 2–128 cm at the center of the anode, transverse dimension varied 4–40 cm	Physical model	Fortin[25]
Bubble coverage (%)		
50–60 (values vary from 24 up to 90)	Physical model	Fortin[25]
65–90	Physical model	Aaberg[33]
50	Physical model	Dewing[35]

energy loss. Therefore, it is essential to remove the gas bubbles beneath the anodes in time. So far, almost all of the works have focused on the bubble-induced electrical resistance[20–25] and bubble behavior[26–35] including bubble coverage at the anode bottom surface, bubble layer thickness and bubble shape etc. Table I lists some parameters of the bubble in cells.

The bubble growth in a laboratory aluminum electrolysis cell was observed by Zhao et al. using a bottom-view transparent cell.[36] Figure 3 shows the formation of a single bubble. The bubble coalescence is believed to be an important source for bubble growth. First, many small bubbles generated on the bottom surface of the anode carbon block. These small bubbles connected to form large bubbles. A bubble grows to a size as large as the anode size before it is released from the anode edge. Furthermore, it's possible that one bubble releases and another bubble is left on the bottom surface. So a single big bubble, may cover one third or half of an anode even a whole anode may form by these two methods.

DESCRIPTION OF THE MODEL

To study the effects of the anode large bubble on current distribution in a cell, a mathematical model based on the following assumptions was developed:

- An anodic large bubble exists at the bottom of anode carbon;
- The bubble position is fixed;
- There is a uniform surface of the cathode carbon block;
- There is a uniform anode–cathode distance;
- There is a uniform anodic current density;
- It is in steady-state condition.

The governing equation for the electrical potential distribution is stated as follows:

$$\nabla[\sigma \nabla V] = 0 \tag{1}$$

where σ is the electrical conductivity, and V is the electrical potential.

The horizontal current is strongly affected by collector bars and current through the cathode carbon into the cathode collector bars is truly three dimensional (3D), therefore, a 3D model is necessary to analyze the electric field in a cell. Because of the symmetry of a cell, only half of the geometric model was chosen as a computational domain. Moreover, the dimensions of the cell such as the cathode carbon and collector bar, and height of the metal, are also significant factors for horizontal current distribution, so the dimensions of the cell are shown in Fig. 4.

In this study, the model was implemented in the commercial software ANSYS. The physical domain was discretized with a structured mesh, which was created by ANSYS Parameter Design Language (APDL). Figure 5 shows the mesh and boundary conditions of the model. The end of the collector bar was chosen as the zero potential and a constant electric current was applied on the anode carbon top surface. Moreover, origin is taken at the center and bottom of the cell. The x-axis, y-axis, and z-axis have been considered along the short side, long side and height of the cell, respectively.

RESULTS AND DISCUSSION

First, a base case without bubbles (case 0) was calculated, then several simulation cases with different bubble coverage or bubble positions were investigated by using the previous model. According to the parameters in Table I, the thickness of the bubble layer was defined as 5 mm and the bubble coverage were chosen as 0%, 33.3%, 50% and 100%, respectively. The simulation cases are presented in Table II.

Horizontal Current Distribution in the Metal Pad Without Bubbles

Figure 6 shows the vector plot of the current in the electrolyte and metal pad. Clearly the current flows vertically across the electrolyte located
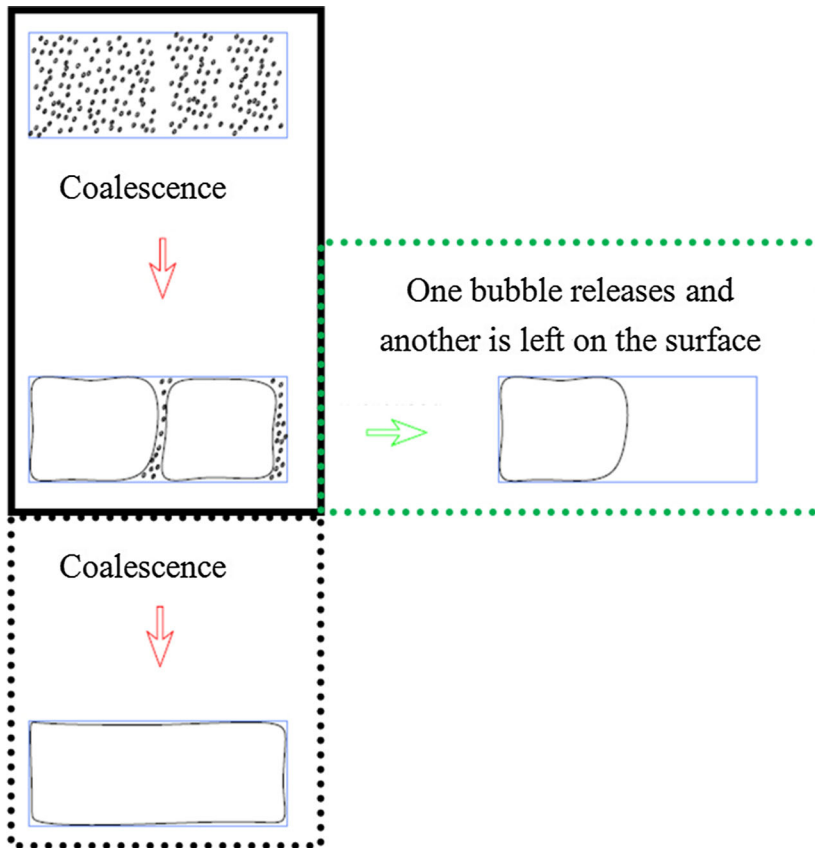
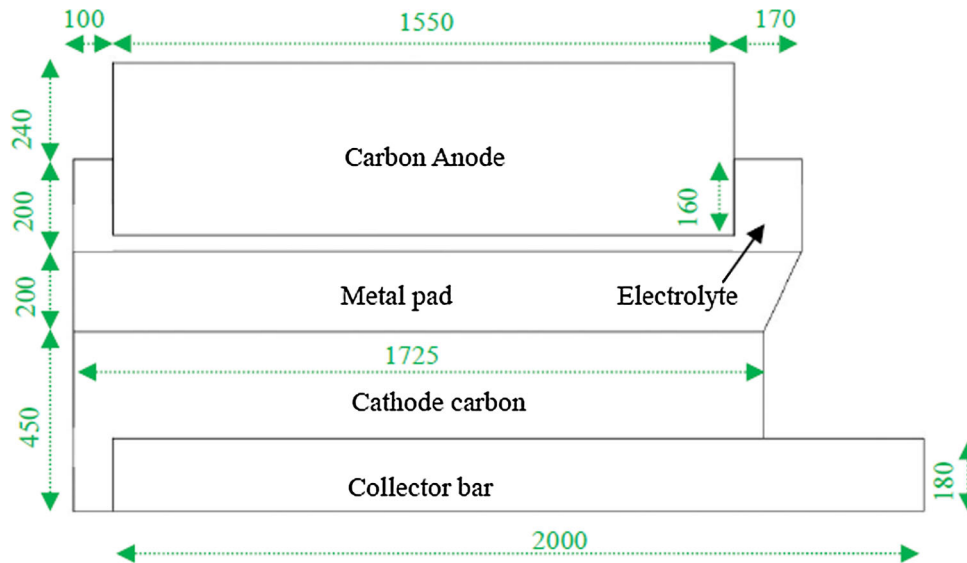Fig. 3. The formation of a single bubble.

Fig. 4. Dimension of an aluminum electrolytic cell (mm).

between the anode and cathode gap. Once the current enters the molten aluminum layer, horizontal currents establish themselves. The current distribution coincides with the results in references,[5,16] indicating that the results using the electric model were reliable.
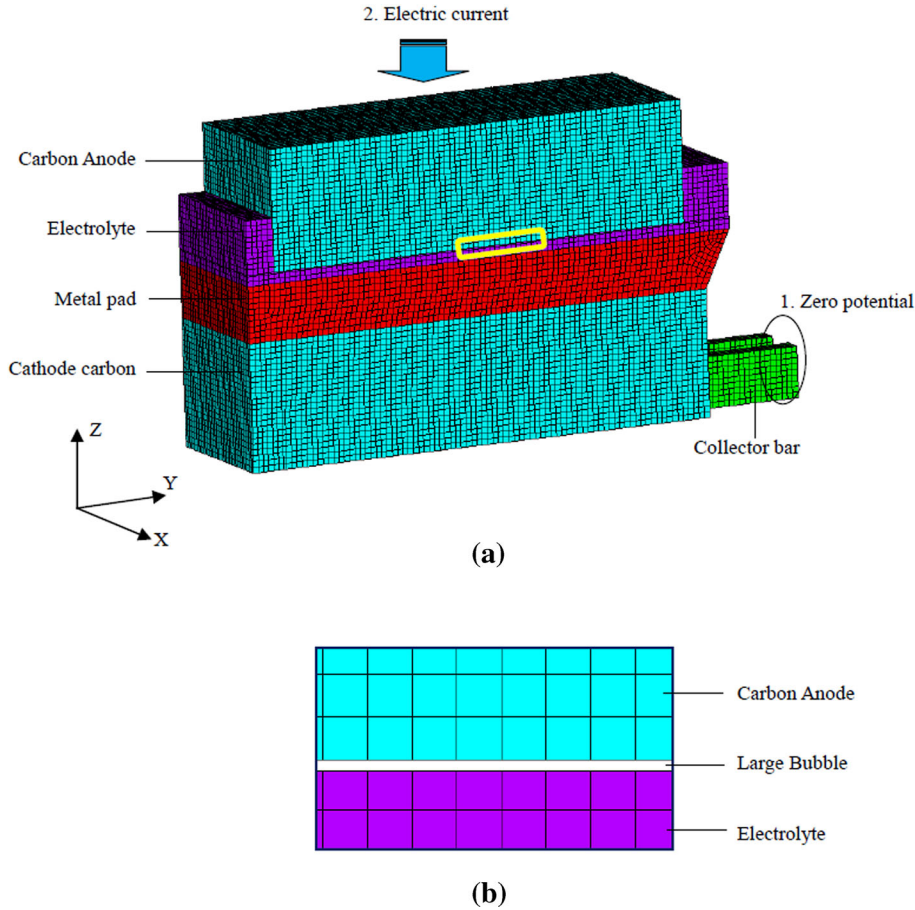
(a)

(b)

Fig. 5. The mesh and boundary conditions of the electric model. (a) full simulation domain, (b) a close up view near the anode-bubble-electrolyte interface.

Table II. Simulation cases with different bubbles

Case no.	Bubble coverage (%)	Bubble position	Bubble thickness (mm)
0	0	/	/
1	33.3	Left side	5
2	33.3	Middle	5
3	33.3	Right side	5
4	50	Left side	5
5	50	Middle	5
6	50	Right side	5
7	100	The whole anode (anode effect)	5

The horizontal current distribution at the upper surface of the metal pad are shown in Fig. 7. Clearly, all of them gradually increase to a maximum value and rapidly decrease to a minimum and the horizontal current is up to 13,844 A m^{-2}, which is situated at about 1.1 m away from cell center.

Effect of Bubble Position

In the model, the bubble was assumed to be fixed. In reality, the bubble generally rolls along the carbon anode surface and escapes around the anode edge. So the effect of the large bubble position on current distribution in the metal pad was conducted in this section. Figure 8 shows the vector plot of the current in the molten aluminum layer with different large bubble positions for a bubble coverage of 33.3%.

Compared with Fig. 6, clearly the current distributions including magnitude and direction of the current have changed so much in Fig. 8. Lots of vertical current and inward current flowing come into being in the metal pad located under or around
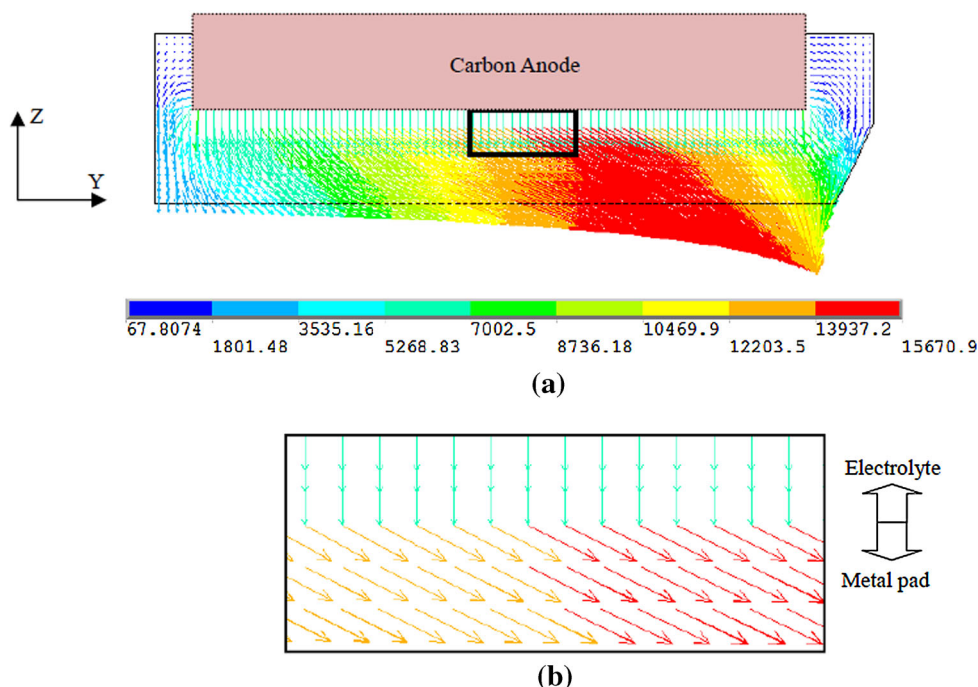
Fig. 6. Vector plot of current in the electrolyte and metal pad, (A m^{-2}). (a) full simulation domain of electrolyte and metal pad, (b) a close-up view near the electrolyte/metal pad interface.

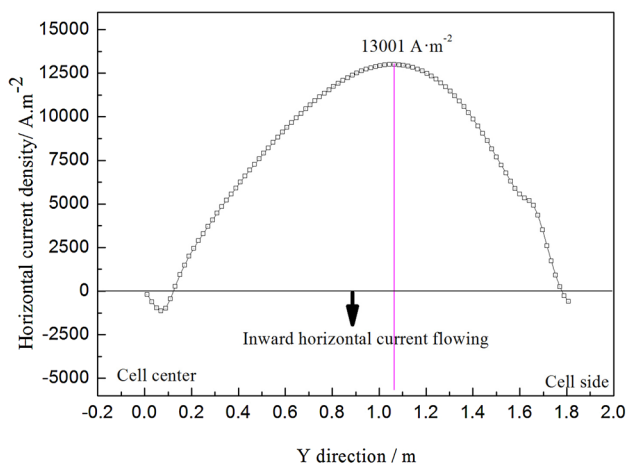Fig. 7. Horizontal current distribution at the upper surface of the metal pad.

the bubble. Zoric et al.[37] and Zhang et al.[24] noted that a local maximum anodic current density appeared close to the bubbles, and the same results have arisen in this study, as shown in cases 1, 2 and 3. Moreover, the closer the bubble is to the cell side (right side), the larger local maximum current density will occur in the metal pad.

Of most interest is the horizontal current because of its adverse effects on the cell current efficiency, energy consumption and cell lifetime. Figure 9 shows horizontal current distribution at the upper surface of the metal pad with different positions of the large bubble for a bubble coverage of 33.3%.

Having compared Fig. 9 with Fig. 7, it's clear that the horizontal current at the upper surface of the metal pad have been greatly converted because of the large bubble introduced in the model: First, when the large bubble is located in the left part bottom of the carbon anode, an inward horizontal current will appears. For example, the inward horizontal current density is up to 8078 A m^{-2} for a bubble coverage of 33.3%; Second, when the bubble varies from the cell center to the cell side, the horizontal current will become larger compared with case 0. The maximum horizontal current density is 20,378 A m^{-2} with a large bubble located in the middle bottom surface of the carbon anode and 30,174 A m^{-2} with a large bubble located in the right bottom surface of the carbon anode (cell side) for a large bubble coverage of 33.3%; The last one is that the peak of horizontal current (the maximum horizontal current density) shifts from the cell center to cell side. The same trend appears for a bubble coverage of 50%, as shown in Fig. 10.

Effect of Bubble Coverage

In this section, the effects of the large bubble coverage on current distribution in the metal pad were investigated. The bubble coverage is controlled by some factors, such as wettability between anode surface and electrolyte, bubble surface tension, and anode surface properties. In a cell, the lower surface of the carbon anode generates small bubbles. These small bubbles will coalescence to form larger bubbles. Some bubbles even grow as big as the anode
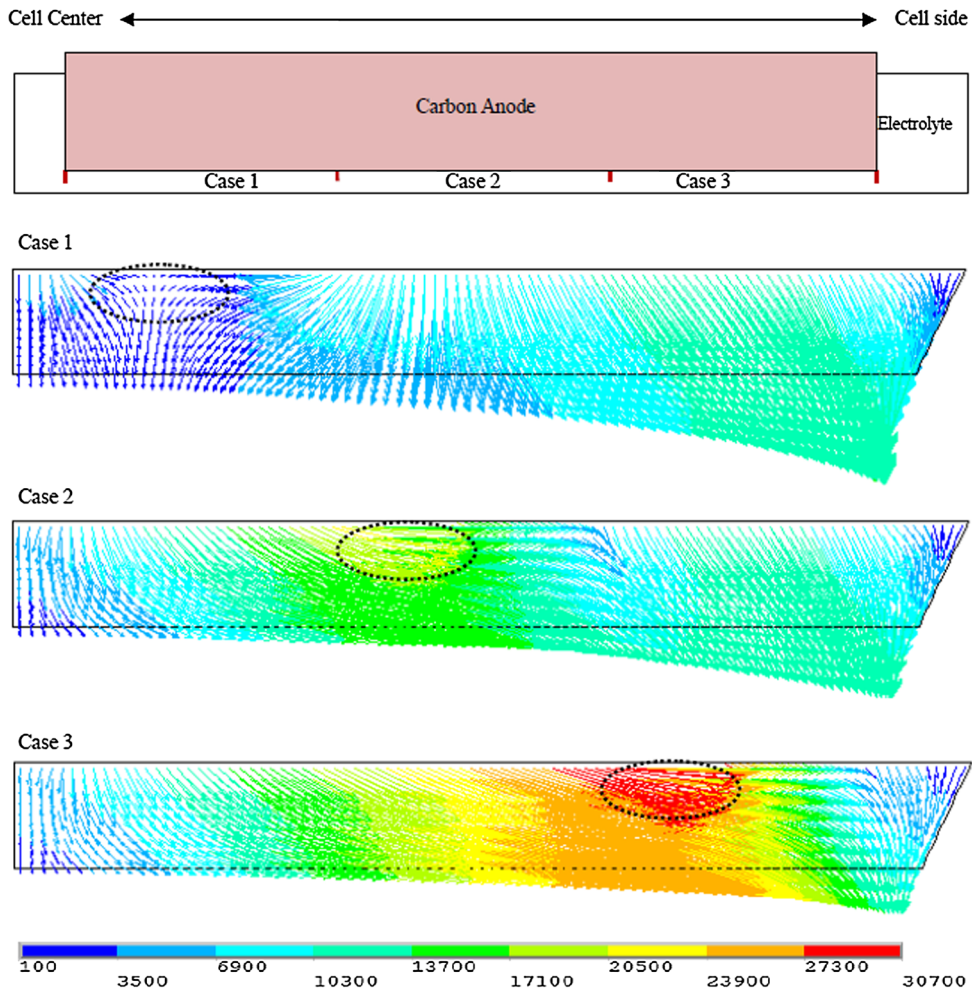
Fig. 8. Vector plot of current in the metal pad with different position of large bubble for a bubble coverage of 33.3%, (A m^{-2}). The bubble in case 1, case 2 and case 3 are located at the left, middle and right bottom surface of carbon anode, respectively.
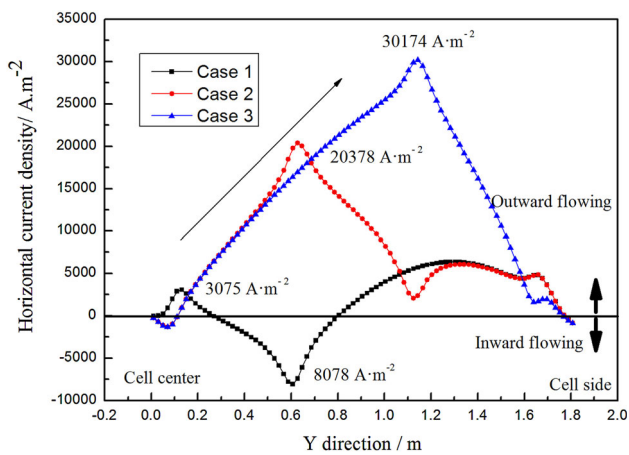

Fig. 9. Horizontal current distribution at the upper surface of the metal pad with different position of large bubble for a bubble coverage of 33.3%. The bubble in case 1, case 2 and case 3 are located at the left, middle and right bottom surface of carbon anode, respectively.
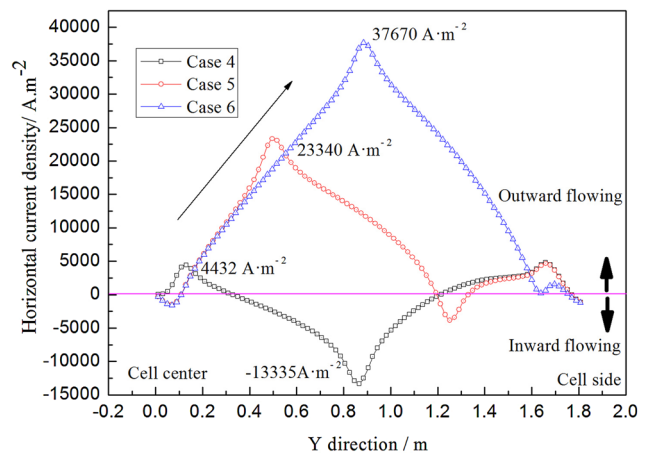

Fig. 10. Horizontal current distribution at the upper surface of the metal pad with different position of large bubble for a bubble coverage of 50%. The bubble in case 4, case 5 and case 6 are located at the left, middle and right bottom surface of carbon anode, respectively.

size, the so-called anode effect. The bubble coalescence is known as an important reason for the bubble growth. Zhao et al.[36] clearly observed the bubble coalescence using a bottom-view transparent cell.

Figure 11 shows the vector plot of the current in the metal pad with different coverage of large bubble for a bubble located in the middle bottom surface of carbon anode. Clearly, the bubble coverage has also a significant impact on the current distributions in the metal pad. Figure 12 demonstrates the horizontal current distributions at the upper surface of the metal pad with different coverage of large bubble for a large bubble located in the middle bottom surface of carbon anode.

First, the maximum horizontal current density increases with increasing bubble coverage. For example, the maximum horizontal current density will increase from 20,378 A m^{-2} to 37,136 A m^{-2} when bubble coverage increases from 33.3% to 100%
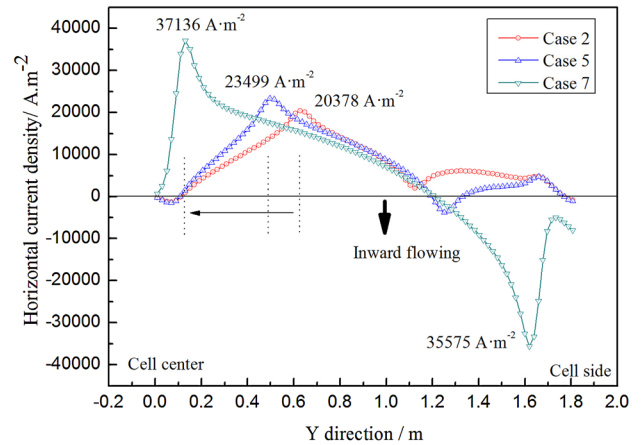

Fig. 12. Horizontal current distribution at the upper surface of the metal pad different large bubble coverage for a bubble located in the middle part of carbon anode. The bubble coverage in case 2, case 5 and case 7 are 33.3%, 50% and 100%, respectively.
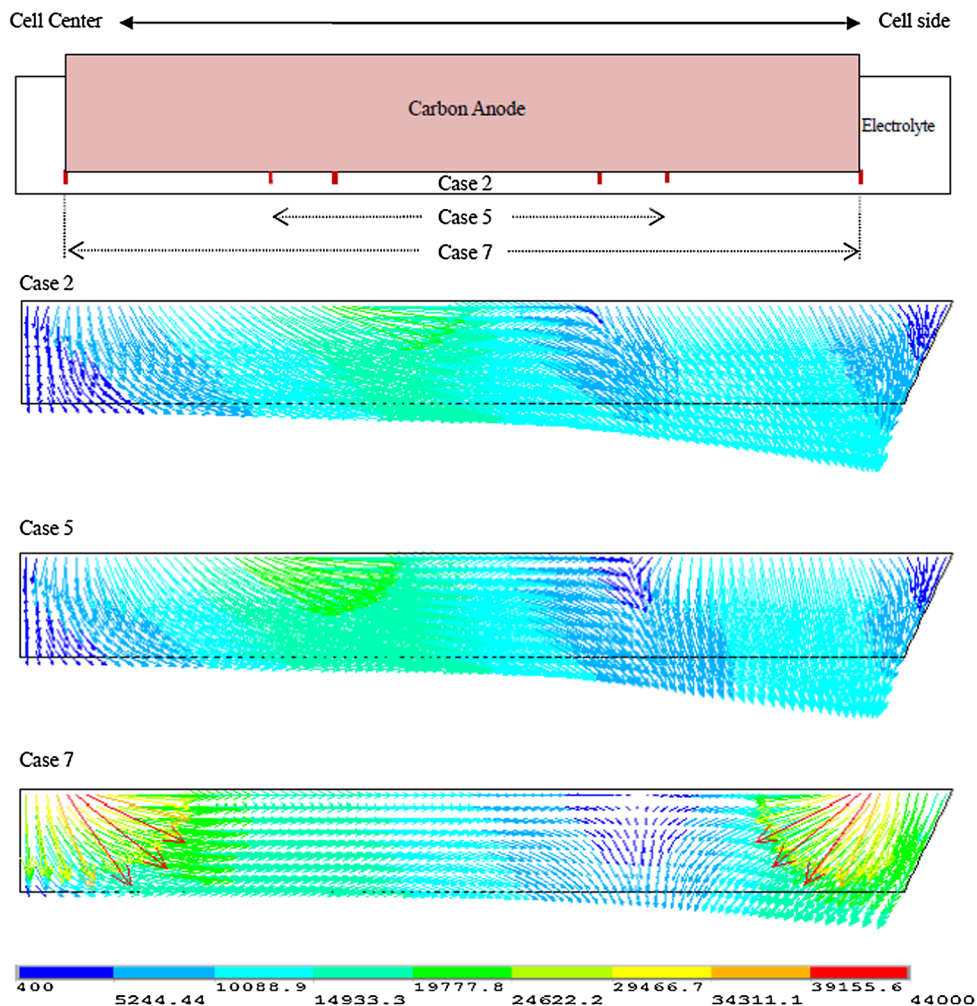

Fig. 11. Vector plot of current in the metal pad with different coverage of large bubble for a bubble located in middle part of carbon anode, (A m^{-2}). The bubble coverage in case 2, case 5 and case 7 are 33.3%, 50% and 100%, respectively.
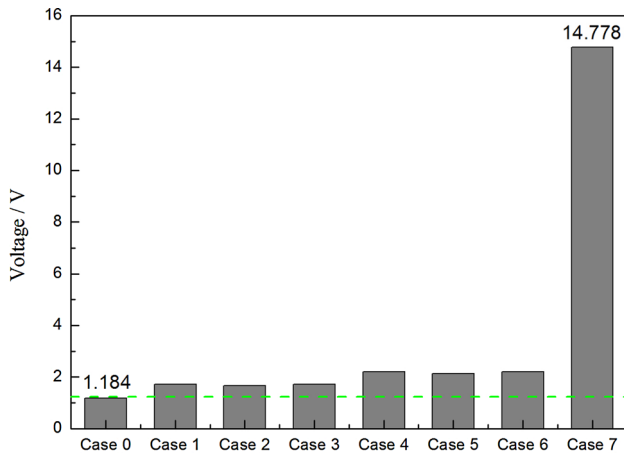
Fig. 13. The electrolyte voltage drop with different bubble coverage and position.

for a bubble located in the middle bottom surface of the carbon anode. Simultaneously, the maximum horizontal current density shifts from the anode center toward the cell center; Second, when the bubble coverage is up to 100%, a large inward horizontal current flowing appears located in the cell side and the maximum inward horizontal current can reach up to 35,575 A m^{-2}. Notably, the large horizontal current will cause an intense fluctuation of the metal pad, so that it can be inferred that the fluctuation will be enhanced during an anode effect.

The voltage is an important parameter for energy consumption. Because the cell voltage difference introduced by the big bubble mainly occurs in the electrolyte, the cell voltage noise is characterized by the electrolyte voltage difference introduced by the big bubble. Figure 13 shows the electrolyte voltage drop with different bubble coverage and positions. Clearly, the bubble has a great influence on electrolyte voltage drop. The predicted voltage drop for a current density of 0.7 A m^{-2} is about 1.184 V for a bubble coverage of 0% and 14.778 V for a bubble coverage of 100%. These value are within the range of experimental measurements reported for industrial cells. Generally, an industrial cell contains multiple anodes, so the current will enter the neighboring anodes if an anode is covered by bubbles. In this article, only one anode was taken into account, and the current into the anode is a constant in the model, so the predicted cell voltage will be a little higher.

CONCLUSION

The effects of an anodic large bubble on the horizontal current in the metal pad of an aluminum electrolytic cell have been numerically investigated using a three-dimensional geometry representative of a cell. The main findings from this study are as follows:

1. The bubble position (for a fixed bubble coverage) significantly influences the local current and horizontal current distribution in the metal pad. When the bubble moves from the cell center to the cell side, the maximum horizontal current density will increase and the location of the maximum horizontal current density shifts from the cell center to the cell side.
2. For a fixed bubble position, the maximum horizontal current increases and the location of the maximum horizontal current density shifts from the anode center to the cell center as the bubble coverage increases.
3. If the whole anode is covered with a large bubble, a large inward horizontal current appears on the cell side. Quantitatively, in such situation, the maximum inward horizontal current can reach up to 35,575 A m^{-2}.

REFERENCES

1. P.A. Davidson and R.I. Lindsay, *J. Fluid Mech.* 362, 327 (1998).
2. A. Furman, *Light Metals 1978*, ed. J.J. Miller (Warrendale, PA: TMS, 1978), pp. 87–106.
3. H. Wintter and K. Lauer, U.S. patent, 3787311 (1974).
4. N.X. Feng, China patent, CN201110385777.0 (2012). (In Chinese).
5. W.J. Tao, T.F. Li, Z.W. Wang, B.L. Gao, Z.N. Shi, X.W. Hu, and J.Z. Cui, *JOM* 67, 929 (2015).
6. Y. Song, N.X. Feng, J.P. Peng, B.K. Li, and Q. Wang, *Light Metals 2015*, ed. M. Hyland (Warrendale, PA: TMS, 2015), pp. 827–830.
7. T. Hudson, J. Huni, V. Potocnik, and D. MacMillan, U.S. patent, 4194959 (1980).
8. W.J. Tao, L. Wang, Z.W. Wang, B.L. Gao, Z.N. Shi, X.W. Hu, and J.Z. Cui, *JOM* 67, 322 (2015).
9. J. McGeer, U.S. patent, 4592820 (1986).
10. M. Gagnon, P. Goulet, R. Beeler, D. Ziegler, and M. Fafard, *Light Metals 2013*, ed. B. Sadler (Warrendale, PA: TMS, 2013), pp. 621–626.
11. D. Townsend, U.S. patent 4795540 (1989).
12. A. Shenyang, Al and Mg Eng. Res. Inst., China Patent CN102453927A (2012) (in Chinese).
13. M. Blais, M. Desilets, and M. Lacroix, *Appl. Therm. Eng.* 58, 439 (2013).
14. K.J. Fraser, D. Billinghurst, K.L.Chen, and J.T. Keniry, *Light Metals 1989*, ed. P.G. Gampbell (Warrendale, PA: TMS, 1989) pp. 219–226.
15. M.F. El-Demerdash, E.E. Khali, H.A. Ahmed, and S. Reda, *Light Metals 1993*, ed. S.K. Das (Warrendale, PA: TMS, 1993) pp. 369–374.
16. X.Q. Qi, N.X. Feng, and J.Z. Cui, *Trans. Nonferrous Met. Soc. China* 15, 931 (2005).
17. Y. Arita and H. Ikeuchi, *Light Metals 1981*, eds. C.J. McMinn, E.M. Adkins, and J.E. Andersen (Warrendale, PA: TMS, 1981), pp. 357–371.
18. R.F. Robl, *Light Metals 1983*, ed. E.M. Adkins (Warrendale, PA: TMS, 1983), pp. 449–456.
19. W.J. Tao, Z.W. Wang, B.L. Gao, Z.N. Shi, X.W. Hu, and J.Z. Cui, *Metalurgija* 53, 311 (2014).

20. M.A. Cooksey, M.P. Taylor, and J.J.J. Chen, *JOM* 51–57 (2008).
21. W. Haupin and H. Kvande, *Light Metals 2000*, ed. R.D. Peterson (Warrendale, PA: TMS, 2000), pp. 379–384.
22. K. Qian and J.J.J. Chen, *J. Appl. Electrochem.* 27, 434 (1997).
23. K. Qian, Z.D. Chen, and J.J.J. Chen, *J. Appl. Electrochem.* 28, 1141 (1998).
24. K.Y. Zhang, Y.Q. Feng, P. Witt, W. Yang, M. Cooksey, Z.W. Wang, and M. Phil Schwarz, *J. Appl. Electrochem.* 44, 1081 (2014).
25. S. Fortin, M. Gerhardt and A.J. Gesing, *Light Metals 1984*, ed. J.P. McGeer (Warrendale, PA: TMS, 1984), pp. 721–741.
26. B.L. Gao, X.W. Hu, J.L. Xu, Z.N. Shi, Z.W. Wang, and Z.X. Qiu, *Light Metals 2006*, ed. T.J. Galloway (Warrendale, PA: TMS, 2006), pp. 467–470.
27. K.Y. Zhang, Y.Q. Feng, P. Schwarz, Z.W. Wang, and M. Cooksey, *Ind. Eng. Chem. Res.* 52, 11378 (2013).
28. Y. Liu, Y.D. Li, T.A. Zhang, and N.X. Feng, *JOM* 66, 1202 (2014).
29. J.L. Xue and H.A. Oye, *Light Metals 1995*, ed. J.W. Evans (Warrendale, PA: TMS, 1995), pp. 265–271.
30. M.A. Cooksey and W. Yang, *Light Metals 2006*, ed. T.J. Galloway (Warrendale, PA: TMS, 2006), pp. 359–365.
31. K.Y. Zhang, Y. Q. Feng, P. Schwarz, M. Cooksey, and Z.W. Wang, *Light Metals 2012*, ed. C.E. Suarez (Warrendale, PA: TMS, 2012), pp. 881–886.
32. Y.Q. Feng, M.A. Cooksey, and P. Schwarz, *Light Metals 2007*, ed. M. Sorlie (Warrendale, PA: TMS, 2007), pp. 339–344.
33. R.J. Aaberg, V. Ranum, K. Williamson, and B.J. Welch, *Light Metals 1997*, ed. R. Huglen (Warrendale, PA: TMS, 1997), pp. 341–346.
34. W.E. Haupin, *Journal of Metals* 23, 46 (1971).
35. E. Dewing, *Can. Met. Quart.* 30, 265 (1991).
36. Z.B. Zhao, Z.W. Wang, B.L. Gao, Y.Q. Feng, Z.N. Shi, and X.W. Hu, *Light Metals 2015*, ed. M. Hyland (Warrendale, PA: TMS, 2015), pp. 801–806.
37. J. Zoric and A. Solheim, *J. Appl. Electrochem.* 30, 787 (2000).